

FIG. 2. Farfield pattern of the amplifier output beam parallel to the active area ( $I=1.4$  A,  $P_{in}=20$  mW).

The single lobed farfield pattern of the amplifier output is shown in Fig. 2. The beam divergence in the plane perpendicular to the active area (measured with a Merchanteck Beamscope) was diffraction limited ( $M^2=1.1$ ). The value of the  $M^2$  parameter parallel to the active area was independent of the amplifier current but increased from 1.3 to 1.5 for an increase in input power from  $30 \mu\text{W}$  to 20 mW. The fact that the beam is not diffraction limited in this plane, indicates that the wave front in the farfield is not planar. We measured the wave front using a wave front profilometer (Melles Griot, WaveAlyzer 13WAS003). As seen from Fig. 3 the wave front is curved in the plane perpendicular to the active layer. This is due to aberrations of the collimating optics. Parallel to the layer the wave front is also curved. This curvature is caused by a change of the refractive index within the active layer due to an inhomogeneous distribution of the temperature and light intensity.

Experiments confirmed that the wavelength and the spectral width of the amplified radiation was identical with those of the oscillator light. The measured spectral amplification bandwidth of the amplifier was about 20 nm. The linewidth of the amplified radiation was 14 MHz.

The radiation generated by this MOPA system was collimated by the lens L3 ( $f=6.5$  mm) and focused by lens L4 ( $f=100$  mm). Mode-matching optics, which consisted of the

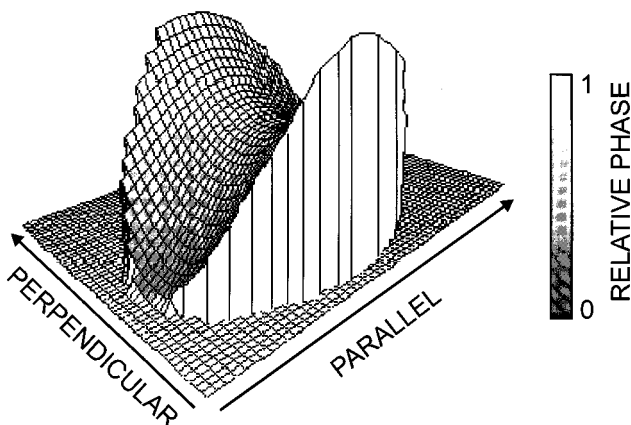


FIG. 3. Relative phase of the wave front of the amplifier output parallel and perpendicular to the active layer.

spherical lenses L5 ( $f=80$  mm) and L8 ( $f=20$  mm) and the cylindrical lenses L6 ( $f=40$  mm) and L7 ( $f=12.5$  mm) focused the laser light into a 4-mirror ring cavity. The MOPA and the ring cavity were optically isolated by a 60 dB isolator (Gsanger, model DLI-1). The crystal (with Brewster cut facets) was placed at the focus between the two spherical mirrors M1 and M2 ( $r=100$  mm). Besides mirror M3 all mirrors were high-reflection (HR) coated for 806 nm. The reflectivities  $R_{HR}$  of the high reflective mirrors were determined by measuring the finesse  $\mathcal{F}$  of a linear cavity formed by two of these mirrors. The finesse of this cavity is given by

$$\mathcal{F} = \frac{\Delta\nu}{\delta\nu} = \frac{\pi\sqrt{R_{HR}}}{1-R_{HR}}. \quad (1)$$

With a measured spectral linewidth  $\Delta\nu=1.5$  MHz and a spectral mode separation  $\delta\nu=15$  GHz, Equation (1) yields a mirror reflectivity of  $R_{HR}=99.97\%$ .

The total losses  $V_c$  of the LBO and BBO crystals (grown by Casteck) were determined by placing them in a linear cavity formed by one of the high reflecting mirrors and by mirror M3 with the reflectivity  $R_{M3}$ . For this cavity the resonant enhancement factor  $\mathcal{E}$  was measured for different values of  $R_{M3}$  ( $R_{M3}=99.7\%$ ,  $99.3\%$ ,  $98.3\%$ ,  $96.1\%$ ). The enhancement factor is given by  $\mathcal{E}=P_{trans}/[(1-R_{HR})P_{OSC}]$ , where  $P_{OSC}$  is the laser power measured in front of M3 and  $P_{trans}$  is 806 nm power transmitted by the HR cavity mirror. In the case of LBO a maximum value of  $\mathcal{E}=86$  was measured for  $R_{M3}=99.3\%$ . For this reflectivity, which provides optimum impedance matching, the total loss in the cavity is identical to the transmission of M3. The crystal losses  $V_c$  are thus given by  $V_c=R_{HR}-R_{M3}-V_{SHG}$ .  $V_{SHG}$  is the power loss due to second harmonic generation. Because the measurements were performed with low laser power ( $P_{OSC}=52$  mW) the value of  $V_{SHG}$  was less than 0.04%. The crystal losses determined in this way from the optimum reflectivity  $R_{M3}$  were 0.6% for LBO and 0.5% for BBO. These low values indicate the high quality of the crystals.

For stable SHG generation the 806 nm diode laser radiation had to be stabilized to a resonance frequency of the external cavity. This was accomplished by coupling the laser radiation transmitted by the ring cavity mirror M4 ( $P<1$  mW) into the oscillator (Fig. 1). This feedback not only locks the wavelength of the oscillator to a resonance of the external cavity but also reduces the oscillator linewidth to less than 10 MHz (the resolution limit of the analyzing scanning Fabry-Perot interferometer). It should be mentioned that the linewidth of the cavity resonance as calculated by taking the losses of the optical components into account is 1.5 MHz. Because of external perturbations, such as mechanical vibrations or acoustic noise, the laser frequency changed to different cavity resonances in time intervals of a few ms to several s. This mode hopping could be strongly reduced by stabilizing the cavity length using a Hansch-Couillaud stabilization scheme.<sup>8</sup>

The output power of the second harmonic radiation generated is shown in Fig. 4 as a function of the laser power. In a 16-mm-long LBO crystal a laser power of 387 mW generated in the crystal 98 mW of 403 nm radiation. This corresponds to a conversion efficiency of  $\eta=25\%$ . The same

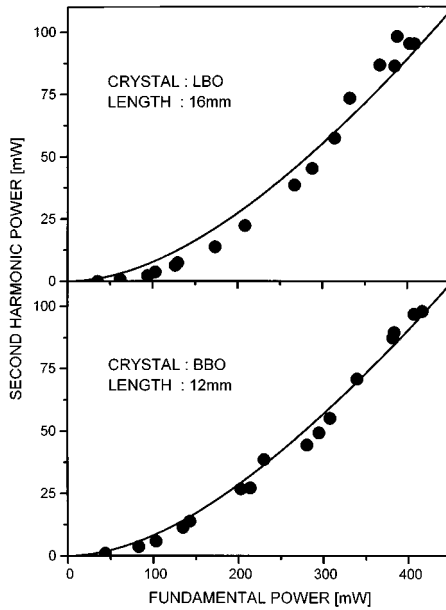


FIG. 4. Power of the generated second harmonic in dependence of the fundamental power.

power was produced in a 12-mm-long BBO crystal with an input power of 417 mW ( $\eta = 24\%$ ). The 20% Fresnel loss at the crystal surface and the 58% loss at mirror M1 (which was not optimized for 403 nm transmission) reduced the power measured outside the cavity to 33 mW. By locking the laser frequency to a cavity mode and stabilizing the cavity length with the Hänsch–Couillaud technique, the power of the second harmonic was stable with  $\Delta P/P \leq 4\%$  over time periods exceeding 500 s.

In the experiment  $\eta_c = 70\%$  of the MOPA radiation was coupled into the  $TEM_{00}$ -mode of the external ring cavity. The radiation resonated in the external cavity was diffraction limited ( $M^2 = 1.0 \pm 0.1$ ). The mode structure of the second harmonic showed in the sagittal plane a  $M^2$  parameter of  $1.1 \pm 0.1$ . Because of the walk-off the  $M^2$  parameter ( $M^2 = 1.4 \pm 0.1$ ) was slightly larger in the tangential plane.

The measured output power and conversion efficiencies are compared with the results of a numerical analysis based on the equations given by Boyd and Kleinman.<sup>6</sup> This analysis starts with a calculation of the second harmonic output assuming an approximate value of the resonant enhancement factor  $\mathcal{E}$  of the ring cavity, where  $\mathcal{E}$  is given by<sup>9</sup>

$$\mathcal{E} = \eta_c \frac{1 - R_{M3}}{(1 - \sqrt{R_{M3}(1 - V_c)})(1 - V_{SHG})R_{HR}^3}^2 \quad (2)$$

With an estimated value of  $\mathcal{E} = 70$  and a laser power of 400 mW the equations of Boyd and Kleinman yield an SHG power of  $P_{SHG} = 54$  mW. This power corresponds to a loss  $V_{SHG} = 0.2\%$ . With this  $V_{SHG}$   $\mathcal{E}$  is calculated. With the obtained value of  $\mathcal{E} = 78$  the power  $P_{SHG}$  is recalculated. This procedure was repeated until the calculated value of  $P_{SHG}$  remained constant. These calculations were performed for laser powers in the range of 40–450 mW.

In a last step the calculated values of  $P_{SHG}$  were fitted to the measured SHG powers using the effective nonlinear coefficient as fit parameter. As seen in Fig. 4 the determined dependence of the SHG output on the laser power is in good agreement with the experimental data. The values obtained for the effective nonlinear coefficients ( $d_{eff} = 0.74$  pm/V for LBO and  $d_{eff} = 2.03$  pm/V for BBO) are also in good agreement with the values of  $d_{eff} = 0.715$  pm/V (LBO) and  $d_{eff} = 2.032$  pm/V (BBO) calculated from the material parameters given in Refs. 10–13.

In summary, efficient frequency doubling of the 806 nm output of an AlGaAs diode laser MOPA system is achieved in critically phase matched LBO and BBO crystals. Up to 98 mW of narrowband 403 nm radiation are generated with an 806 nm laser power of 400 mW. This corresponds to a crystal internal conversion efficiency of 25%. The laser frequency was locked to a resonance of the external cavity by optical feedback. With additional active cavity length control stable oscillation of the laser diode on one of the cavity resonance frequencies was achieved. Under these conditions the power fluctuations of the generated frequency doubled 403 nm radiation were less than 4%.

Higher power levels of the frequency doubled output are expected for higher laser power. Higher laser power was in fact generated by further amplifying the MOPA output in a broad area amplifier (SDL-S9439-C, Temperature  $-20^\circ\text{C}$ , 8.0 A). This amplifier generated 2.85 W in a beam with a  $M^2$  parameter of 1.1 and 1.6 perpendicular and parallel to the active layer, respectively. Calculations indicate that for this laser power the SHG output power should well exceed the half-watt level.

This research was supported by the Ministry of Education, Science, Research and Technology of Germany under Contract No. 13 N 6379 8.

<sup>1</sup>S. Nakamura, M. Senoh, S. Hagahama, N. Iwasi, T. Yamada, T. Matsushita, H. Kiyoku, and Y. Sugimoto, *Jpn. J. Appl. Phys.* **1** *35*, 74 (1996).

<sup>2</sup>C. Zimmermann, V. Vuletic, A. Hemmerich, and T. Hänsch, *Appl. Phys. Lett.* **66**, 2318 (1995).

<sup>3</sup>I. Biaggio, P. Kerkoc, L. Wu, P. Gunter, and B. Zysset, *J. Opt. Soc. Am. B* **9**, 507 (1992).

<sup>4</sup>L. Hesselink, in *Conference Proceedings of the Annual Meeting, IEEE Lasers and Electro-Optics Society* (Institute of Electrical and Electronics Engineers, New York, 1993), p. 82.

<sup>5</sup>W. Wang, M. Fejer, R. Hammond, M. Beasley, C. Ahn, M. Bortz, and T. Day, *Appl. Phys. Lett.* **68**, 729 (1996).

<sup>6</sup>G. Boyd and D. Kleinman, *J. Appl. Phys.* **39**, 3597 (1968).

<sup>7</sup>E. Gehrig, B. Beier, K.-J. Boller, and R. Wallenstein (unpublished).

<sup>8</sup>T. Hänsch and B. Couillaud, *Opt. Commun.* **35**, 441 (1980).

<sup>9</sup>A. Ashkin, G. Boyd, and J. Dziedzic, *IEEE J. Quantum Electron.* **2**, 109 (1966).

<sup>10</sup>K. Kato, *IEEE J. Quantum Electron.* **22**, 1013 (1986).

<sup>11</sup>J. Fan, R. Eckardt, R. Byer, C. Chen, and A. Jiang, *IEEE J. Quantum Electron.* **25**, 1196 (1989).

<sup>12</sup>S. Lin, Z. Sun, B. Wu, and C. Chen, *J. Appl. Phys.* **67**, 634 (1990).

<sup>13</sup>B. Wu, F. Xie, C. Chen, D. Deng, and Z. Xu, *Opt. Commun.* **88**, 451 (1992).